Effective and Equivalent Refractive Index Models for Patterned Solar Cell Films via a Robust Homogenization Method

Ekin Gunes Ozaktas, Sreyas Chintapalli, and Susanna M. Thon

Electrical and Computer Engineering, Johns Hopkins University, Baltimore, 21218, USA

Solar cells containing complex geometric structures such as texturing, photonic crystals, and plasmonics are becoming increasingly popular, but this complexity also creates increased computational demand when designing these devices through costly full-wave simulations. Treating these complex geometries by modeling them as homogeneous slabs can greatly speed up these computations. To this end, we introduce a simple and robust method to solve the branching problem in the homogenization of metamaterials. We start from the branch of the complex logarithm in the Nicolson-Ross-Weir method with the minimum absolute mean derivative in the low frequency range and enforce continuity. This is followed by comparing the reflectance, transmittance, and absorptance of the original and homogenized slabs. We use our method to demonstrate accurate and fast optical simulations of patterned PbS colloidal quantum dot solar cell films. We also compare patterned solar cells homogenized via equivalent models (wavelength-scale features) and effective models (sub-wavelength-scale features), finding that for the latter, agreement is almost exact, whereas the former contains small errors due to the unphysical nature of the homogeneity assumption for that size regime. This method can greatly reduce computational cost and thus facilitate the design of optical structures for solar cell applications.

I. INTRODUCTION AND BACKGROUND

Complex geometries such as photonic crystals, plasmonic structures, and textured surfaces have gained popularity in solar cell design. However, the full-wave simulations required to study 2D/3D structures are computationally costly. In this work, we use effective and equivalent material models to homogenize patterned layers and reduce the problem to 1D, for which methods such as the Transfer Matrix Method (TMM) can be used. Once a homogenized model is produced, it can be reused in many simulations, reducing the computational cost drastically. Unlike equivalent models, effective models have an averaged electric field similar to that in the inhomogeneous medium, since the feature size (f.s.) of the inhomogeneities satisfies f.s. $\ll \lambda$, and homogenization is physically valid. In equivalent models f.s. $\approx \lambda$, and effects such as diffraction and scattering dominate [1].

Homogenizing complex materials simplifies their treatment. Many works use homogenization to model electrical properties of solar cells with multiple constituents [2]. Others use effective media to model complex geometries, such as textured [3], silicon nanowire [4], and plasmonic solar cells [5]. Many solar cell patterns satisfy f.s. $\approx \lambda$, necessitating a thorough investigation of equivalent models, which are insufficiently treated in the literature.

A popular homogenization method is the Nicolson-Ross-Weir (NRW) method, which starts from the S-parameters to obtain the refractive index $N_{\rm eff}(\omega) = n_{\rm eff}(\omega) + i\kappa_{\rm eff}(\omega)$ of a corresponding homogeneous slab. $\kappa_{\rm eff}(\omega)$ can be uniquely calculated but $n_{\rm eff}(\omega)$ depends on a complex logarithm with multiple branches indexed by the integer branch number m [6]-[8]. The ambiguity of m results in a branching problem, which must be resolved. One approach takes m at each frequency such that $n_{\rm eff}(\omega)$ is closest to the application of the Kramers-Kronig relations to $\kappa_{\rm eff}(\omega)$. This can result in discontinuities, so a different approach is based on continuity [6], [9], but this leaves the starting branch ambiguous. It is common to start from the zeroth branch for a low enough frequency, since the slab is optically thin [1].

Some works consider an effective thickness $d_{\rm eff}$ different from the geometric thickness. One definition involves boundaries for which the incoming and outgoing waves are plane waves (which is not true near an inhomogeneous material) [6]. Another treatment rounds the branch number calculated from the Kramers-Kronig relations for permittivity and permeability and takes effective thickness as the value that minimizes the error associated with the rounding [10].

II. METHODS

We now introduce our solution to the branching problem. First, we obtain the S-parameters via finite-difference timedomain (FDTD) simulation [11] of the inhomogeneous material. Then we must choose the starting branch. Since the low-frequency behavior of $N_{\text{eff}}(\omega)$ of a wide range of materials will approach a constant, and since the branches differ by $2\pi m/k_0 d_{\rm eff}$ (k_0 is the free space wavenumber), for low frequencies (small k_0d_{eff}), the false branches become very steep while the correct branch is flat in comparison. Thus, we find the starting branch by minimizing the magnitude of the mean derivative across the low frequency portion of each branch (before the first discontinuity). Then, we use the continuity of $n_{\text{eff}}(\omega)$ for the remaining frequencies: for each point, the next branch index is recursively taken as that yielding the closest value to the present branch. This method is more robust than that commonly found in the literature, which starts from a low enough frequency to ensure that the slab is optically thin and thus takes the first branch index as 0. This is a "hard" requirement: that method fails if the starting branch is not 0 in reality. However, our method only has a "soft" condition that the correct branch be flat enough to be distinguishable, and thus the starting branch number can be nonzero.

Next, we analytically calculate the reflectance ($R_{\rm eff}$), transmittance ($T_{\rm eff}$), and absorptance ($A_{\rm eff}$) of the homogenized slab. We compare these to $R_{\rm inh}$, $T_{\rm inh}$, $A_{\rm inh}$ from the FDTD simulation of the inhomogeneous material via mean squared error (MSE). We choose $d_{\rm eff}$ to minimize MSE. This improves matching of the optical spectra, especially for equivalent models, due to the greater region where plane wave behavior breaks down when effects such as diffraction dominate.

III. RESULTS AND DISCUSSION

We first demonstrate the steps of our method in Fig. 1 with a 790 nm thick homogeneous slab of PbS colloidal quantum dots (PbS CQDs) with exciton peak at 1200 nm. The agreement between the optical spectra from the FDTD calculation and our method is exact (MSE = 1.68×10^{-6}), verifying the self-consistency of our model. The refractive index of PbS CQDs was obtained via Variable Angle Spectroscopic Ellipsometry (VASE).

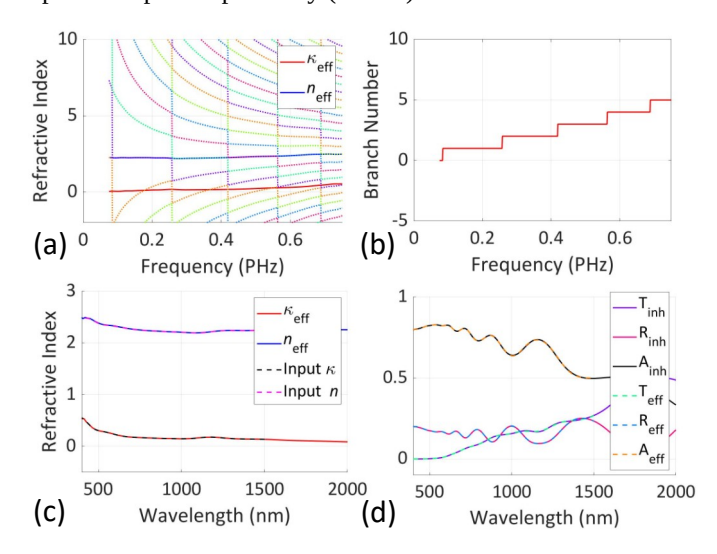


Fig. 1. The index model estimation method applied to a homogeneous slab of PbS CQDs. (a) Branches of the complex logarithm together with the real and imaginary parts of the refractive index; (b) branch number as a function of frequency; (c) extracted refractive index compared to the known refractive index of the PbS CQD (since it is homogeneous); (d) optical behavior from the FDTD simulation compared to the method of this work.

A more interesting example is an inhomogeneous material with f.s. $\approx \lambda$ so that assuming homogeneity is unphysical. Here, we want an equivalent slab model with the same R, T, and A as the inhomogeneous material. We investigate a PbS CQD film nanodisk array with ZnO filling the space in between. The nanodisks have radius 252.8 nm with periodicity 632 nm, and height 790 nm. The refractive index of ZnO was obtained from [12]. As visible in Fig. 2, the effective thickness of the homogenized slab is thicker than the geometric thickness due to the surrounding lack of plane wave behavior.

We also apply the Kramers-Kronig relations to $\kappa_{\rm eff}(\omega)$, observing they are violated especially for shorter λ . However, this does not violate causality [13]. For an effective model, the averaged electric field in the inhomogeneous material corresponds to that in the homogenized one, and the Kramers-Kronig relations hold [13]. However, this is not so for equivalent models. Rather, it simply demonstrates that the homogenization process for f.s. $\approx \lambda$ is physically unjustified, resulting in an "unphysical" equivalent index model.

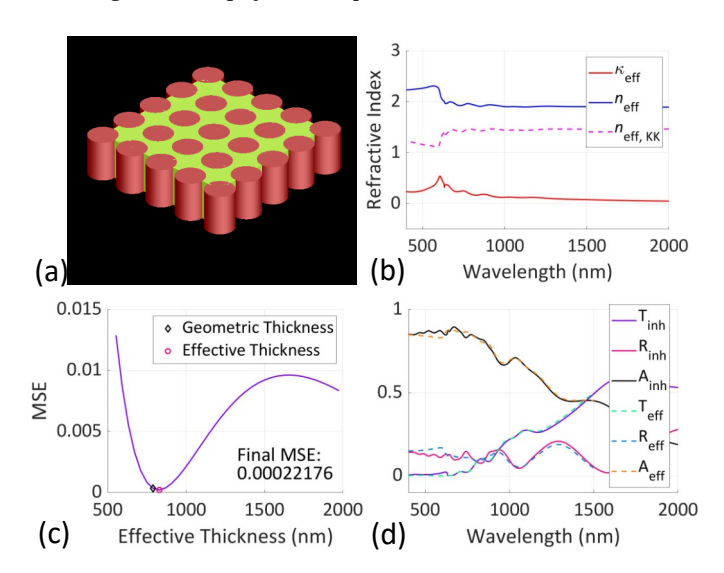


Fig. 2. Demonstration of the method for a patterned slab of PbS CQD nanodisks surrounded by ZnO. (a) The inhomogeneous structure with PbS CQDs (red) and ZnO (green); (b) the equivalent refractive index model with Kramers-Kronig relations; (c) MSE as a function of effective thickness; (d) comparison of the optical spectra.

We now simulate the behavior of a PbS CQD solar cell. Modifying the design in [14], the solar cell is composed of 225 nm of ITO as the front contact, 75 nm of ZnO, the above 790 nm slab of nanodisks, 100 nm of PbS CQDs, and 300 nm of Au as an electrode. The refractive indices of ITO and Au were obtained from [15], [16]. We replace the patterned layer by the equivalent slab calculated previously. Then we simulate the solar cell using a fast optical stack solver [11]. We compare the results to the FDTD simulation. We also compare (Fig. 3) with a solar cell that is identical except that the radius of nanodisks is 25.28 nm and the periodicity of the structure is 63.2 nm, for which f.s. $\ll \lambda$, and the homogenized medium is an effective model. As we might expect, for the solar cell simulated with an effective model, the comparison of FDTD to the stack solution is almost exact for the entire wavelength range of interest, due to the physically viable homogeneity assumption. However, for the solar cell simulated with an equivalent model, there is more error due to the unfounded assumption of homogeneity, and the dominance of effects such as diffraction and scattering that cannot be modeled with a homogeneous slab. Regardless, both simulations are substantially accurate and much faster than an FDTD simulation, running almost instantaneously.

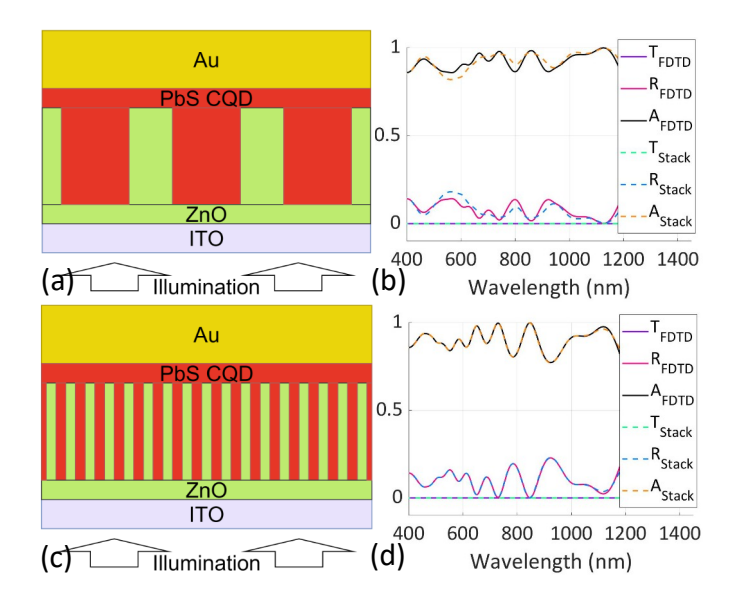


Fig. 3. Comparison of the optical behavior of the solar cell under consideration depending on simulation technique. (a) depicts a solar cell which was simulated with an equivalent model and (b) the corresponding FDTD results compared to the optical stack solver, while (c) contains the solar cell for which an effective model was used and (d) contains the optical behavior comparison.

IV. CONCLUSION

In this work, we have introduced a simple and robust solution to the branching problem in the NRW method that starts from the branch of the complex logarithm with the lowest absolute mean derivative in the low frequency region, and enforces continuity to recursively obtain the remaining branch numbers. We then compare the reflectance, transmittance, and absorptance of the homogenized and inhomogeneous slabs, and minimize the deviations between them to calculate the effective thickness of the homogenized slab. We investigate two regimes. When f.s. $\ll \lambda$, (i) the homogenization is physically valid, (ii) the averaged electric field in the inhomogeneous and effective models is the same [13], (iii) the optical behavior between the two agree, and (iv) the Kramers-Kronig relations hold. Meanwhile, in the regime with wavelength-scale features, these properties do not hold due to the unphysical homogeneity assumption. Regardless, an equivalent model giving the same optical behavior is still useful in simplifying complex models. We demonstrate this by reducing a patterned solar cell to a 1D problem and solving for its optical properties much more quickly than with FDTD simulations, thus improving computational efficiency during photovoltaic design. We expect that this model will be widely useful to the field in helping researchers design optical structures for a variety of solar cell applications.

ACKNOWLEDGEMENTS

We would like to acknowledge the National Science Foundation (ECCS-1846239) for funding this work.

REFERENCES

- [1] S. Arslanagic, T. V. Hansen, N. A. Mortensen, A. H. Gregersen, O. Sigmund, R. W. Ziolkonski, and O. Breinbjerg, "A review of the scattering-parameter extraction method with clarification of ambiguity issues in relation to metamaterial homogenization," *IEEE Antennas and Propagation Magazine*, vol. 55, pp. 91–106, 2013.
- [2] G. Richardson, C. P. Please, and V. Styles, "Derivation and solution of effective medium equations for bulk heterojunction organic solar cells," *Euro. Jnl of Applied Mathematics*, vol. 28, pp. 973–1014, 2017.
- [3] S. Rowlands, J. Livingstone, and C. Lund, "Optical modelling of thin film solar cells with textured interfaces using the effective medium approximation," *Solar Energy*, vol. 76, pp. 301–307, 2004.
- [4] H. Wang, X. Liu, L. Wang, and Z. Zhang, "Anisotropic optical properties of silicon nanowire arrays based on the effective medium approximation," *International Journal of Thermal Sciences*, vol. 65, pp. 62–69, 2012.
- [5] Y. A. Akimov, K. Ostrikov, and E. P. Li, "Surface plasmon enhancement of optical absorption in thin-film silicon solar cells," *Plasmonics*, vol. 4, pp. 107–113, 2009.
- [6] X. Chen, T. M. Grzegorczyk, B.-I. Wu, J. Pacheco, and J. A. Kong, "Robust method to retrieve the constitutive effective parameters of metamaterials," *Physical Review E*, vol. 70, no. 016608, 2004.
- [7] Z. Szabo, G.-H. Park, R. Hedge, and E.-P. Li, "A unique extraction of metamaterial parameters based on Kramers– Kronig relationship," *IEEE Transactions on Microwave Theory* and Techniques, vol. 58, pp. 2646–2653, 2010.
- [8] G. Angiulli and M. Versaci, "Retrieving the effective parameters of an electromagnetic metamaterial using the Nicolson-Ross-Weir method: An analytic continuation problem along the path determined by scattering parameters," *IEEE Access*, vol. 9, pp. 77511–77525, 2021.
- [9] Y. Shi, Z.-Y. Li, L. Li, and C.-H. Liang, "An electromagnetic parameters extraction method for metamaterials based on phase unwrapping technique," *Waves in Random and Complex Media*, vol. 26, pp. 417–433, 2016.
- [10] S. Yoo, S. Lee, J.-H. Choe, and Q-H. Park, "Causal homogenization of metamaterials," *Nanophotonics*, vol. 8, pp. 1063–1069, 2019.
- [11] Ansys, "Ansys Lumerical Photonics Simulation and Design Software," www.ansys.com/products/photonics.
- [12] O. Aguilar, S. De Castro, M. P. F. Godoy, and M. R. Sousa Dias, "Optoelectronic characterization of Zn_{1-x}Cd_xO thin films as an alternative to photonic crystals in organic solar cells," *Optical Materials Express*, vol. 9, pp. 3638–3648, 2019.
- [13] A. Alu, A. D. Yaghjian, R. A. Shore, and M. G. Silveirinha, "Causality relations in the homogenization of metamaterials," *Physical Review B*, vol. 84, no. 054305, 2011.
- [14] T. Kim, X. Jin, J. H. Song, S. Jeong, and T. Park, "Efficiency limit of colloidal quantum dot solar cells: Effect of optical interference on active layer absorption," ACS Energy Letters, vol. 5, pp. 248–251, 2020.
- [15] T. A. F. Konig, P. A. Ledin, J. Kerszulis, M. A. Mahmoud, M. A. El-Sayed, J. R. Reynolds, and V. V. Tsukruk, "Electrically tunable plasmonic behavior of nanocube–polymer nanomaterials induced by a redox-active electrochromic polymer," *ACS Nano*, vol. 8, pp. 6182–6192, 2014.
- [16] P. B. Johnson and R. W. Christy, "Optical constants of the noble metals," *Phys. Rev. B*, vol. 6, pp. 4370–4379, 1972.